Population genomic analysis of elongated skulls reveals extensive female-biased immigration in Early Medieval Bavaria

Krishna R. Veeramah[a], Andreas Rott[b,1], Melanie Groß[c,1], Lucy van Dorp[d], Saioa López[e], Karola Kirsanow[c], Christian Sell[c], Jens Blöcher[c], Daniel Wegmann[f,g], Vivian Link[f,g], Zuzana Hofmanová[f,g], Joris Peters[b,h], Bernd Trautmann[b], Anja Gairhos[i], Jochen Haberstroh[j], Bernd Päffgen[k], Garrett Hellenthal[d], Brigitte Haas-Gebhard[i], Michaela Harbeck[b,2,3], and Joachim Burger[c,2,3]

[a]Department of Ecology and Evolution, Stony Brook University, Stony Brook, NY 11794-5245; [b]State Collection for Anthropology and Palaeoanatomy, Bavarian Natural History Collections, 80333 Munich, Germany; [c]Palaeogenetics Group, Institute of Organismic and Molecular Evolution, Johannes Gutenberg University Mainz, 55099 Mainz, Germany; [d]UCL Genetics Institute, Department of Genetics, Evolution and Environment, University College London, WC1E 6BT London, United Kingdom; [e]Cancer Institute, University College London, WC1E 6DD London, United Kingdom; [f]Department of Biology, University of Fribourg, 1700 Fribourg, Switzerland; [g]Swiss Institute of Bioinformatics, 1700 Fribourg, Switzerland; [h]ArchaeoBioCenter and Institute for Palaeoanatomy, Domestication Research and the History of Veterinary Medicine, Ludwig Maximilian University, 80539 Munich, Germany; [i]Bavarian State Archaeological Collection, 80538 Munich, Germany; [j]Bavarian State Department of Monuments and Sites, 80539 Munich, Germany; and [k]Institute of Prehistoric and Protohistoric Archaeology, Ludwig Maximilian University, 80799 Munich, Germany

Edited by Eske Willerslev, University of Copenhagen, Copenhagen, Denmark, and approved January 30, 2018 (received for review November 21, 2017)

Modern European genetic structure demonstrates strong correlations with geography, while genetic analysis of prehistoric humans has indicated at least two major waves of immigration from outside the continent during periods of cultural change. However, population-level genome data that could shed light on the demographic processes occurring during the intervening periods have been absent. Therefore, we generated genomic data from 41 individuals dating mostly to the late 5th/early 6th century AD from present-day Bavaria in southern Germany, including 11 whole genomes (mean depth 5.56×). In addition we developed a capture array to sequence neutral regions spanning a total of 5 Mb and 486 functional polymorphic sites to high depth (mean 72×) in all individuals. Our data indicate that while men generally had ancestry that closely resembles modern northern and central Europeans, women exhibit a very high genetic heterogeneity; this includes signals of genetic ancestry ranging from western Europe to East Asia. Particularly striking are women with artificial skull deformations; the analysis of their collective genetic ancestry suggests an origin in southeastern Europe. In addition, functional variants indicate that they also differed in visible characteristics. This example of female-biased migration indicates that complex demographic processes during the Early Medieval period may have contributed in an unexpected way to shape the modern European genetic landscape. Examination of the panel of functional loci also revealed that many alleles associated with recent positive selection were already at modern-like frequencies in European populations ∼1,500 years ago.

paleogenomics | demographic inference | population genetics | Early Medieval | Migration Period

Europe experienced a profound cultural transformation between Late Antiquity and the Middle Ages that laid the foundations of the modern political, social, and religious landscape. During this period, colloquially known as the "Migration Period," the Roman Empire gradually dissolved, with 5th and 6th century historiographers and contemporary witnesses describing the formation and migration of numerous Germanic peoples, such as the Goths, Alamanni, Gepids, and Longobards. However, the genetic and social composition of groups involved and the exact nature of these "migrations" are unclear and have been a subject of substantial historical and archaeological debate (1).

In the mid 6th century AD, the historiographer Jordanes and the poet and hagiographer Venantius Fortunatus provide the first mention of a group known as the Baiuvarii that resided in modern day Bavaria. It is likely that this group had already started to form in the 5th century AD, and that it emanated from a combination of the romanized local population of the border province of the former Roman Empire and immigrants from north of the Danube (2). While the Baiuvarii are less well known than some other contemporary groups, an interesting archaeological feature in Bavaria from this period is the presence of skeletons with artificially deformed or elongated skulls (Fig. 1*A*).

Artificial cranial deformation (ACD), which is only possible during early childhood, is a deliberate and permanent shaping of the head performed with great effort. In some societies reshaping the human skull has been seen as an ideal of beauty, while it

Significance

Many modern European states trace their roots back to a period known as the Migration Period that spans from Late Antiquity to the early Middle Ages. We have conducted the first population-level analysis of people from this era, generating genomic data from 41 graves from archaeological sites in present-day Bavaria in southern Germany mostly dating to around 500 AD. While they are predominantly of northern/central European ancestry, we also find significant evidence for a nonlocal genetic provenance that is highly enriched among resident Early Medieval women, demonstrating artificial skull deformation. We infer that the most likely origin of the majority of these women was southeastern Europe, resolving a debate that has lasted for more than half a century.

Author contributions: K.R.V., M.G., K.K., B.H.-G., M.H., and J. Burger designed research; K.R.V., A.R., M.G., L.v.D., S.L., C.S., D.W., B.T., G.H., M.H., and J. Burger performed research; K.R.V., J.P., A.G., J.H., B.P., and B.H.-G. contributed new reagents/analytic tools; K.R.V., A.R., M.G., L.v.D., S.L., C.S., J. Blöcher, V.L., Z.H., and J. Burger analyzed data; and K.R.V., A.R., M.G., L.v.D., D.W., G.H., B.H.-G., M.H., and J. Burger wrote the paper.

The authors declare no conflict of interest.

This article is a PNAS Direct Submission.

Data deposition: Mitochondrial genome sequences and genomic data have been deposited in the European Nucleotide Archive, https://www.ebi.ac.uk/ena [accession no. PRJEB23079 (BAM format)].

[1]A.R. and M.G. contributed equally to this work.

[2]M.H. and J. Burger contributed equally to this work.

[3]To whom correspondence may be addressed. Email: Michaela.Harbeck@extern.lrz-muenchen.de or jburger@uni-mainz.de.

This article contains supporting information online at www.pnas.org/lookup/suppl/doi:10.1073/pnas.1719880115/-/DCSupplemental.

Published online March 12, 2018.

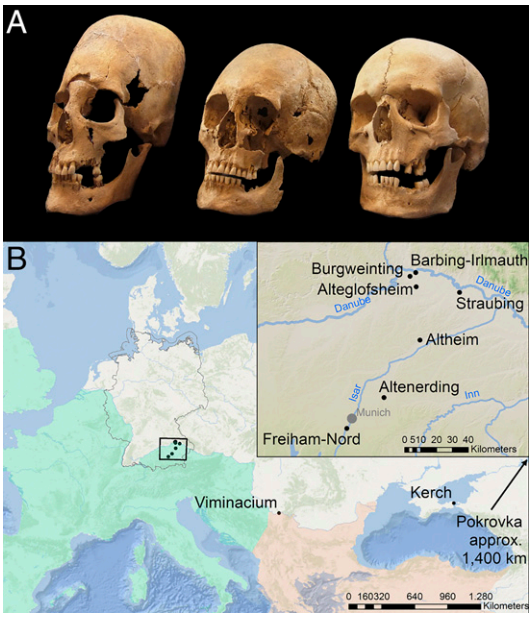

Fig. 1. (*A*) Investigated skulls with strong (*Left*, AED_1108) intermediate, (*Middle*, STR_220), and no (*Right*, AED_92) skull deformation. (*B*) Location of archaeological sites from which genomes were analyzed ($n = 41$) on a map of Europe with today's borders of Germany and the former borders of the western (green) and the eastern (light brown) Roman Empire. Bavarian sample sites (black square) are shown in the *Inset*. Sites in detail (number of deformed/nondeformed skulls): Altenerding (3/7), Alteglofsheim (1/0), Altheim (0/4), Barbing-Irlmauth (1/1), Burgweinting (1/1), and Straubing (3/9). Five additional individuals from Straubing were defined as intermediate. In addition, reference sites are given with which the Bavarian, Medieval genome data were compared: FN_2 (Freiham near Munich, ∼300 AD), deformed skull VIM_2 (Viminacium in Serbia, ∼550 AD), deformed skull KER_1 (Kerch on the Crimea, 256–401 cal AD), and two Sarmatians PR_4 and PR_10 (Pokrovka in southern Russia, 5th–2nd century BC).

may also have acted as a marker of status, nobility, or affiliation to a certain class or group (3). While ACD is a worldwide phenomenon that was practiced at least up to the 20th century (4), during the Late Roman and Early Medieval period in Europe it is most popularly associated with the Huns, an ambiguously defined nomadic group thought to have migrated into Europe from Asia (5). However, the earliest evidence for ACD appears in Europe in 2nd century AD burials in present day Romania that predate the proposed Hunnic invasion (6).

Interestingly, there is a striking difference in the practice of ACD in the east and west of the continent: in eastern European burials, ACD is found at much higher frequency [50–80% of skulls in Hungary versus less than 5% in western graveyards] and is equally common among males and females and across all age classes (*SI Appendix*, Figs. S50–S52). In contrast, in Bavarian burials of the late 5th/early 6th century AD and elsewhere in western Europe, this cultural phenomenon is restricted to mainly adult females, while not noted in children and juveniles (*SI Appendix*, Fig. S53). Some scholars suggest these patterns are consistent with adult women migrating from eastern Europe or even Asia into western Europe (6). However, the associated assemblages of grave goods for women in the west with ACD cannot be clearly differentiated from non-ACD burials, leading others to argue that the practice was culturally adopted in western Europe from eastern foreign traditions (7).

To examine support for either of these two scenarios we produced genomic data for 36 adults of both sexes from six Bavarian cemeteries located within the former Roman Empire dating around 500 AD (Fig. 1*B*). All samples were selected with the explicit intent that they would belong to a single generation, and 14 of them demonstrated possible ACD. In addition, we produced genomic data from a local Roman soldier as well as four individuals from further east (including two deformed skulls from the 4th–6th century) that may have acted as a source of origin for people with ACD migrating west.

Results

Data Generation. We identified 36 archaeological samples from six different Early Medieval cemeteries in Bavaria (Fig. 1 and *SI Appendix*, Table S1), dating roughly from the middle of the 5th to the middle of the 6th century AD, that were suitable for genomic analysis based on high endogenous DNA content (mean 48.43%, 10.41–72.64%), high complexity of DNA libraries, evidence of postmortem damage consistent with ancient DNA (8), and low estimates of contamination (calculated from blank controls: mean 0.15%, 0.004–1.25%; and mitochondrial contamination rate: mean 1.12%, 0.006–7.09%). For comparison, we additionally examined the following five samples: FN_2 (around 300 AD) from Munich that appears to be a Roman soldier (cf. *SI Appendix*, section 1), KER_1 (3rd–4th century AD) from Crimea associated with Ostrogoth material culture, VIM_2 (6th century AD) from Serbia associated with Gepid material culture, and two Sarmatian-associated samples from the site Pokrovka from the Southern Urals in Russia (PR_4 and PR_10, 5th–2nd century BCE). Both KER_1 and VIM_2 had skull deformation, while PR_4 and PR_10 are expected to possess common genetic ancestry with migrants from the Steppe that could have acted as a source for ACD in Europe.

All 41 samples underwent targeted capture and sequencing using an array that targeted ∼5,000 putatively unlinked neutral loci, each containing primarily 1,000 bp of contiguous sequence (henceforth referred as the 5-Mb neutralome) as well as 486 SNP loci of known phenotypic association. We obtained a mean coverage of 72× at the 5-Mb neutralome with a range of 13× to 147× across the 41 samples. Excluding the two samples with <20× coverage (STR_328 = 16×, PR_4 = 13×), we were able to obtain transition–transversion ratios close to the expected value of 2.1 when calling genotypes using a model that incorporates postmortem damage (9). In addition, 11 of these samples (including KER_1, VIM_2, and FN_2) underwent additional whole genome sequencing (WGS) (mean depth 5.56×, 2.26×–13.27×, *SI Appendix*, Table S6).

Archaeological Context. All Early Medieval Bavarian burials investigated were dated either by archaeological finds and/or a combination of ^{14}C dates and grave goods (*SI Appendix*, Table S1). Nine of these samples (all women based on comparisons of relative X chromosome to autosomal read depth) showed clear signals of skull deformation, while the status of skull deformation was questionable for 5 samples (4 women and one man, referred to henceforth as "intermediate"). Of the remaining 22 samples with normal skull shape, 13 were women. We note that STR_502 was later found to date two generations later than other samples from the cemetery. Some females with ACD could be argued to demonstrate grave assemblages associated with an eastern context (STR_328, AEH_1), but others were not specific (NW_54) or were common in the area under investigation (e.g., STR_535). A putative eastern context can be observed in some of the individuals without ACD as well (e.g., STR_266). None of the graves with ACD show any anomalies regarding burial custom (10). Two samples from Straubing both considered to have an intermediate skull shape (STR_355, female and STR_491, male) were shown to be siblings. As the former had higher coverage, the latter was excluded from any population-based analysis of the ancient samples.

Geographical Origin and Genetic Diversity. A principal component analysis (PCA) of our ancient genomic data against that from a variety of modern reference population samples using both haploid and diploid datasets, as well as a supervised model-based clustering of the diploid data found that all men and 11 of the 13 women with normal skull shape clustered among modern

POPULATION BIOLOGY

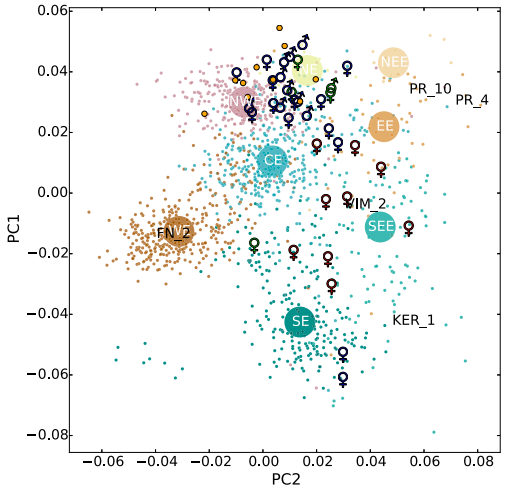

Fig. 2. Procrustes-transformed PCA of ancient samples using pseudohaploid calls based on off-target reads using an imputed POPRES modern reference dataset. Blue, green, and red male or female symbols are ancient Bavarian individuals with normal, intermediate, and elongated skulls, respectively. Orange circles are Anglo-Saxon era individuals. Large circles are medians for regions, dots are individuals. CE, central Europe; EE, eastern Europe; NE, northern Europe; NEE, northeastern Europe; NEW, northwestern Europe; SE, southern Europe; SEE, southeast Europe; WE, western Europe. Percentage of variation explained by PCs 1 and 2 for modern populations only is 0.25% and 0.15%.

northern and central European individuals (Figs. 2 and 3). Additional analyses examining patterns of haplotype sharing using only ancient whole genomes with coverage >10× also showed a high degree of matching to northern/central Europe relative to the alleged Roman soldier FN_2 (*SI Appendix*, Fig. S49), and as a group, both sexes with normal skull shape were closest (as assessed by F_{ST} on diploid 1-kb haplotypes) to modern 1000 Genomes samples of northern and western European Ancestry (CEU) (*SI Appendix*, Table S37).

A population assignment analysis (PAA) at the level of individual modern nation states suggested greatest genetic similarity of these normal-skulled individuals with modern Germans, consistent with their sampling location (Fig. 4 *A* and *B* and *SI Appendix*, Table S35). The only exceptions to this general pattern of northern/central European ancestry were the two women, STR_300 and STR_502, which were of a more southern ancestry associated with present day Greece and Turkey, respectively (*SI Appendix*, Fig. S29).

A much more diverse ancestry was observed among the females with elongated skulls, as demonstrated by a significantly greater group-based F_{IS} (*SI Appendix*, Fig. S35). All these females had varying amounts of genetic ancestry found today predominantly in southern European countries [as seen by the varying amounts of ancestry inferred by model-based clustering that is representative of a sample from modern Tuscany, Italy (TSI), Fig. 3], and while the majority of samples were found to be closest to modern southeastern Europeans (Bulgaria and Romania, Fig. 4*C*), at least one individual, AED_1108, appeared to possess ∼20% East Asian ancestry (Fig. 3), which was also evident from the high number of haplotypes within the 5-Mb neutralome that were private to modern East Asian 1000 Genomes individuals (EAS), while also demonstrating an overall ancestry profile consistent with Central Asian populations (*SI Appendix*, Fig. S33). No modern European individual from the Simons Genome Diversity Panel (SGDP) (11) showed any evidence of significant East Asian ancestry except one Hungarian individual with less than 5%. A higher amount of East Asian ancestry was inferred for AED_1108 than all modern Caucasus and Middle Eastern individuals, and 28 of 33 South Asian individuals.

From the individuals of intermediate skull size, one female (STR_310) exhibited the same southern European ancestry profile found in most other females with clear skull deformation, while the remaining four clustered clearly within northern/central Europeans (*SI Appendix*, Fig. S30). In addition, while females with normal skulls generally exhibited the same northern/central European component as the males (excluding STR_300 and STR_502), a small but significant East Asian component was consistently inferred for ALH_3.

A diverse ancestry was also inferred for the two non-Bavarian samples with elongated heads. KER_1 from Ukraine possessed significant southern European ancestry as well as South Asian ancestry, with an overall profile that best matched modern Turkish individuals. The Gepid VIM_2 from Serbia demonstrated a similar Central Asian-like genetic profile to the Medieval Bavarian AED_1108 with an even larger East Asian component and number of private haplotypes but with less southern European/Middle Eastern ancestry (*SI Appendix*, Figs. S31 and S33). The two Sarmatian individuals (PR_4 and PR_10) fitted a general eastern European/western Asian profile, but also possessed a much larger northern European component [as represented by modern Finnish individuals (FIN)] similar to modern Russians, consistent with their sampling location. As previously observed in Schiffels et al. (12) contemporary Anglo-Saxon samples appeared to be primarily of northern/central European ancestry, with greatest similarity overall to modern British and Scandinavian individuals (*SI Appendix*, Fig. S32).

A signal of population structure among our ancient samples was also observed when no modern reference samples were used to orientate genomic ancestry. An unsupervised model-based clustering analysis with $K = 2$ (*SI Appendix*, Fig. S27) essentially reiterated the results using the supervised analysis that identified individuals with predominantly northern/central versus southern European ancestry, while an outlier analysis identified STR_502, VIM_2, PR_10, KER_1, and AED_1108 as significantly distinct from all of the other samples, consistent with their significant non-European ancestry when orienting them with modern reference populations.

It was also notable that no Bavarian individual (normal or ACD, male or female) possessed ancestry related to southwestern Europe, as represented by a sample of individuals sequenced from the Iberian population in Spain (IBS). This is in contrast to the Roman soldier dating to around 300 AD sampled from the same region, for which its largest ancestry component was IBS, with greatest genetic similarity to modern Spanish and southern French individuals (*SI Appendix*, Fig. S31). Based on an analysis of patterns of haplotype sharing, the Roman soldier (FN_2: 11.08×) was found to have substantially more southern European, West Asian, and Middle Eastern ancestry than two normal-skulled Early Medieval Bavarians with high genomic coverage (ALH_10: 12.17×, ALH_1: 13.27×) (*SI Appendix*, Figs. S48 and S49).

Phenotypic Analysis. Along with the 5-Mb neutralome, we enriched 486 loci (mean 52×, 8×–174×, coverage calculated excluding X/Y chromosomal positions) that have been associated with specific phenotypes (including certain physiological functions) (*SI*

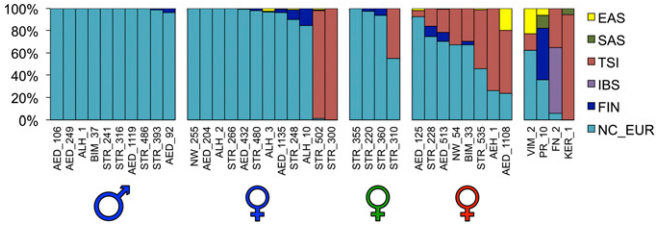

Fig. 3. Supervised model-based clustering ADMIXTURE analysis for ancient samples based on phased haplotypes for individual 1,000 bp loci from the 5-Mb neutralome. Analysis is based on the best of 100 runs for $K = 8$, but NC_EUR is the ancestry summed across 1000 Genomes CEU, 1000 Genomes GBR, and GoNL populations (i.e., it represents a northern/central European ancestry). Blue, green, and red male or female symbols are ancient Bavarian individuals with normal, intermediate, and elongated skulls, respectively.

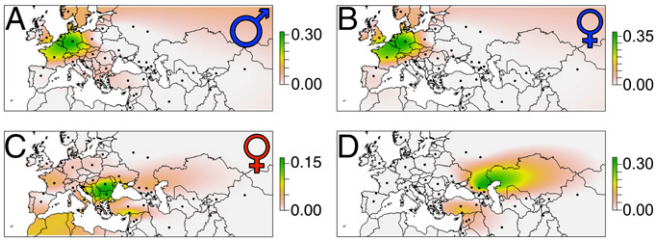

Fig. 4. Geographic distribution of population assignment analysis (PAA) results on pseudohaploid calls from off-target reads summed across individuals for (*A*) all Bavarian males, (*B*) all Bavarian females with normal skulls, (*C*) all Bavarian females with elongated skulls, and (*D*) KER_1 and VIM_2.

Appendix, section 7), many of which are thought to have changed frequencies in human populations over the last 10,000 y due to adaptation to different environments and changing diet. Based on the HIrisPlex system (13), the majority (~80%) of individuals with normal or intermediate skulls (and thus northern/central European ancestry) showed high probabilities for blue eyes and blonde hair (*SI Appendix*, Fig. S7 *A* and *B*); in contrast, the majority of women with deformed skulls had a high likelihood for brown eyes (80% of individuals), and both brown and blonde hair (~60% and 40% of individuals, respectively) were represented in the sample.

When examining the 13910*T allele associated with lactase persistence, the nondeformed group possessed allele frequencies (0.571; 95% CI 0.422–0.721) similar to modern central Europeans, while individuals with deformed skulls exhibited lower frequencies (0.278; 95% CI 0.071–0.485); in this respect, they more closely resemble present-day southern Europeans (14) (*SI Appendix*, Fig. S7*C*). We note that even as recently as the Bronze Age this allele was found at less than 10% in Europe (15), providing a fairly narrow window of ~2,000 y within which the lactase persistence phenotype must have rapidly increased in frequency on the continent.

It has previously been suggested that a network of inflammatory disease-risk alleles was under positive selection in Europeans recently, potentially in response to *Yersinia pestis* pandemics (16). However, despite our Bavarian population living well before the time of the Black Death and even just before the first recorded instance of bubonic plague, i.e., the Justinian plague in eastern Europe, at all three analyzed loci the allele frequencies of the supposedly protective derived alleles are similar to that in modern European populations (*SI Appendix*, Fig. S7*D* and Table S30). The allele frequencies at seven other loci associated with common inflammatory diseases, such as Crohn's disease, type 1 diabetes, multiple sclerosis, and celiac disease, are also not distinguishable in the Medieval sample from those in modern Europeans, fitting well with Raj et al.'s (16) expectations that allele frequency changes at these loci occurred due to selection more than 5,000 y ago.

Parameterizing Recent European Population Growth. Multiple population genetic studies have inferred that Europeans have undergone recent explosive population growth of 1–4% per generation (17, 18), with estimates of the start of this growth ranging from 3.5 to 9.5 thousand years ago (kya). In addition, archaeologists have inferred that central Europe has experienced a general trend of population growth starting in the Early Medieval through to modern times (19). In this respect, our sample is chronologically well suited to calibrate the course of European population demography. We estimated an allele frequency spectrum (AFS) for the male and female individuals with normal skull formation (excluding STR_300 and STR_502) at our 5-Mb neutralome and found an excess of singletons, which would be consistent with European growth beginning at least before the age of our ancient population. We used ∂a∂i (20) to fit a two-dimensional AFS (2D-AFS) consisting of our ancient Bavarian population and 492 chromosomes from modern Dutch individuals (21) to a demographic model containing recent exponential growth (22) as well as continuity between the ancient and modern Dutch (GoNL) populations. In addition, we took advantage of the fixed time in years separating the two populations (1.5 ky) to simultaneously estimate the per generation mutation rate, μ, rather than having to convert our parameter estimates into real-world units using an assumed rate. We estimated that growth began 5.9 kya (95% CI 4.4–10.4 kya) with a growth rate of 1.81% (95% CI 1.00–2.36%) and an estimate of μ of 1.14×10^{-8} (95% CI 6.51×10^{-9}–1.53×10^{-8}), the latter of which is very much in line with recent WGS pedigree estimates (23) as well as another AFS-based estimate (18).

Discussion

Dynamics of Female Mobility. The most striking result of this study is the genetic difference between Early Medieval individuals buried in Bavaria with and without ACD. While both males and females with normal skulls were found to be a largely homogenous set of individuals with a common northern/central European ancestry (with two exceptions STR_300 and STR_502), females with deformed skulls sampled from the same cemeteries were very genetically diverse, demonstrating a wide range of both modern northern/central and southern/southeastern European ancestry, and even some samples with East Asian ancestry.

If the structure of modern genetic variation can be considered a suitable proxy for how genetic variation was approximately structured in Europe and the rest of Eurasia 1,500 y ago, then local Medieval Bavarian individuals were probably not practicing ACD with their own children. Instead, consistent with the suggestion of Hakenbeck (6), adult females with deformed skulls found in Medieval Bavaria likely migrated from southeastern Europe, a region that not only contains the earliest known European burials of males and females with ACD but also the largest accumulation (*SI Appendix*, Figs. S51 and S52). It also seems unlikely that mass migration of people from the southeast were involved, as there appears to be no major impact on the local Bavarian gene pool (ACD samples make up only a very small percentage of the local burials). Instead, given that ACD was a particularly involved and labor-intensive procedure that may indicate a certain role or status in Medieval society, these females may have moved as part of a system in which local Bavarian communities practiced exogamy to form strategic alliances with entities to the east.

The diversity of the genomic profile of the immigrant females with ACD suggest two primary models with regard to how, who, and to what extent these central European peoples interacted with people from the east. In the first, local populations in Early Medieval Bavaria may have had direct contacts with an extremely diverse set of people practicing ACD, ranging from southeastern European tribes such as the Gepids to those with probably even more Asian origins that moved into Europe such as Huns, which would explain the presence of East Asian ancestry in AED_1108 and possibly STR_328 and ALH_3. Alternatively, this pool of women may have origins exclusively in southeast Europe and more precisely the middle or lower Danube Basin area, which itself contained a long-standing mixture of people and where the custom of creating elongated skulls arose both locally and from interactions with groups from the east (not only Huns, but also predating Sarmatians and Alans), similar to the model proposed by Molnár et al. (24). The similar Central Asian genomic profiles of AED_1108 from Bavaria and VIM_2 from 6th century Serbia support this second scenario.

While the immigrant females would have been clearly distinguishable physically among the local population based on the combination of their enlarged crania as well as their different eye, hair, and perhaps even skin pigmentation patterns, it is noteworthy that their assemblies of grave goods appear to reflect both local customs and more distant material cultures (10). This not only indicates a potentially significant level of integration of these women into local life, but also cautions against inferring migration from material culture alone.

A Hunnic Spread for Skull Deformation in Europe? The question arises of whether the observed East Asian ancestry in both our late 5th/early 6th century Bavarian and Serbian samples is consistent

with an assumed ultimate Hunnic origin of skull deformation in both eastern and western Europe. Generally, it is assumed that the Huns were a diverse mixture of east European and Central Asian people, and that they integrated men and women from the local populations during their westward expansion (25).

Located ∼1,600 km away from VIM_2 and predating both this sample and AED_1108 by at least a century, our most easterly sampled deformed skull is KER_1 from the Crimea. The age of the sample and its archaeological context associate the skull with the Ostrogoth people but also with the ancient Greek city of Pantikapaion, which it is said was destroyed by the Huns in 370 AD (*SI Appendix*, section 1). Thus, we might hypothesize an exclusive "Hunnic" origin of skull deformation spreading from the Steppe and into Europe would be reflected in Central/East Asian ancestry in KER_1 similar to AED_1108 and VIM_2. However, KER_1 provided no evidence of such ancestry. Instead, it displays similarities to today's Mediterranean populations, consistent with this being a Greek trading colony founded in the 6th century BCE. While clearly more samples are needed to support this assessment, the absence of any Central/East Asian ancestry in KER_1 but a significant proportion observed in AED_1108 and VIM_2 is nevertheless surprising and not in line with an exclusive Central/East Asian origin of ACD.

As a further "proxy" for a potential eastern origin of the individuals with ACD, we analyzed Sarmatian-associated genomes from southern Russia (400 BC). While there is some genetic evidence of an East Asian ancestry in these samples, it is limited and much less than that estimated in both AED_1108 and VIM_2. Their largest additional ancestry component is represented by modern Finnish individuals (much of which likely reflects their previously observed Yamnaya-like ancestry) (26), which is very low in all our other ancient samples (normal and deformed skulls). Overall we found no evidence for a higher amount of East Asian-related ancestry in the 10 deformed skull individuals relative to 29 individuals without deformed skulls (Wilcoxon rank-sum test two-sided P value = 0.84). When coupled with archaeological evidence of skull deformation in Romania as early as the 2nd century, it perhaps suggests any Hunnic or earlier Sarmatian-like influence in spreading the tradition of ACD from the Steppe may have been low, and their genetic impact even lower.

Lack of Mediterranean and Gallo-Roman Influence on Medieval Bavarian Genetic Structure. Excluding individuals with ACD and two women with Greek/Anatolian ancestry, our samples from Early Medieval Bavaria can be genetically characterized as typically northern/central European. It is perhaps surprising that no local individual was found to share recent common genetic ancestry with a Roman soldier living in the same area ∼200 y earlier. The analysis of his genome identifies him to be of southwest European origin. Thus, our results, though only based on one sample, argue against significant admixture between any Roman populations from more southern parts of the former Roman Empire and our individuals buried in Bavaria around 500 AD.

Conclusion

The population genomic analysis of Early Medieval people from cemeteries in the area of modern day Bavaria provide clear evidence of female-biased long-distance migration and consequently more diverse ancestry of women versus men in this specific context. In addition, through our high coverage capture approach, we were able to obtain population-level allele frequencies (and generate an ancient human AFS) that allowed us to (*i*) establish that many disease-risk alleles previously thought to have emerged relatively recently were already well established in northern/central Europe by around 500 AD, and (*ii*) that explosive population growth likely began during the Chalcolithic period of central Europe. In general, our results emphasize that, unlike when investigating more ancient prehistoric periods where just a few samples can reveal major events, obtaining dense local samples from across Europe will be essential to better understand the complex patterns of migration, admixture, population structure, growth, and selection during more recent times.

Methods

Ancient DNA Extraction, Library Preparation, and Screening. Sample preparation was conducted in dedicated ancient DNA facilities as already described in Scheu et al. (27) with slight modifications. Quality assessment for all samples is based on library complexity measured by quantitative real-time PCR (9) and calculation of endogenous content after shallow sequencing on Illumina MiSeq. Detailed screening results are listed in *SI Appendix*, Table S2.

Capture Assay and WGS. Neutral Region Explorer (NRE) (28) was used to identify 4,687 independent neutral 1-kb autosomal loci suitable for in-solution capture and short-read sequencing, based on an initial list of 37,574 loci (29). This set of loci were supplemented with 429 regions of 500 bp and 486 phenotypic informative markers. A MYbaits custom target enrichment kit (MYcroarray) was used for capturing. For detailed description of the assay see *SI Appendix*, section 3. Additionally, 11 samples were whole genome shotgun sequenced. Sequencing was performed on Illumina platforms. All sequenced reads were processed as described previously (9). Haploid and diploid genotype calling was performed, accounting for postmortem damage as previously described (9).

Ancient DNA Authenticity. Postmortem damage was assessed using mapDamage 2.0 (30). Contamination was estimated from the mitochondrial capture data using the approach of Fu et al. (31) and for all male shotgun data using ANGSD (32) (*SI Appendix*, section 8 and Table S34).

Modern and Ancient Reference Samples. We performed demographic analysis of our ancient samples using two main approaches. In the first, we capitalized on our high coverage at the 5-Mb neutralome by phasing individual (1 kb) haplotypes based on diploid calls using PHASE (33), with 1000 Genomes Eurasian populations (34), high-coverage SGDP (11), Turkish (35), and Dutch GoNL (21) samples used as modern reference populations. In the second, we took advantage of the high endogenous content of our samples to obtain haploid calls based on off-target reads that overlapped SNPs found in imputed European (POPRES) (36) and Eurasian SNP-array (HellBus) (37) datasets. The 1000 Genomes Eurasian (34), SGDP (11), and contemporary Anglo-Saxon genomes (12) were also included in these analyses.

Principal Component Analysis. PCA was conducted using smartpca (38). When analyzing the off-target calls, individual pseudohaploid PCAs were conducted for each ancient sample separately, and then individual analyses were combined using a Procrustes transformation in R using the vegan package. When analyzing data from the 5-Mb neutralome, each distinct 1-kb haplotype from each of the ∼5,000 regions was coded as a distinct biallelic SNP allele and all samples were analyzed simultaneously (38).

Model-Based Clustering. Model-based clustering analysis was applied in two different ways to the 1-kb haplotypes from the 5-Mb region. In the first, a supervised analysis was performed on the ancient samples and the SGDP genomes using ADMIXTURE (39) with the following reference populations: 1000 Genomes CEU, GBR, IBS, TSI, FIN, along with SAS and EAS and GoNL. In addition, we performed an unsupervised analysis only for the 38 ancient samples using STRUCTURE (40) allowing for correlated allele frequencies.

PAA. We adapted a previously described likelihood-based approach (41) for determining the most likely population of origin for a sample to our haploid SNP data, allowing ancient samples to be from any modern reference population with at least 10 individuals. To account for uncertainty, we performed 100 5-Mb nonoverlapping block bootstrap replicates. We visualized this uncertainty on a geographic map of Eurasia using interpolation.

Allele and Haplotype Sharing Patterns. We used CHROMOPAINTER (42) to summarize DNA patterns in each ancient individual as a "sharing profile" consisting of the inferred proportion of DNA for which that individual is most closely related ancestrally to individuals from each of K modern groups. We generated these sharing profiles conditional on analyzing either (*i*) each SNP independently ("allele sharing profile") or (*ii*) each SNP conditional on neighboring SNPs ("haplotype sharing profile") (9). For *ii*, we used PHASE (33) or SHAPEITv2 (43) to phase all individuals jointly. We calculated these sharing profiles for each ancient and modern individual independently, with the modern populations used (and hence K) varying

across datasets, and performed jack-knifing across chromosomes to assess uncertainty. See *SI Appendix*, section 16 for further details.

Outlier Analysis. We first treated our 38 usable ancient samples as a single population. We then determined the likelihood that each sample in turn belonged to this single population by estimating the probability of observing a particular pair of haplotypes, given the population haplotype frequencies. Outliers were considered those samples with an empirical P value <0.001 based on a null distribution of likelihoods (*SI Appendix*, section 12).

F_{IS} and F_{ST} Analysis. F_{IS} and F_{ST} were estimated across the individual 1-kb loci for groups of ancient samples and modern populations using the estimators of Nei (44) and Bhatia et al. (45), respectively. SEs and 95% CIs were constructed by performing 100 bootstraps for individual loci.

Allele Frequency Spectrum Analysis. A joint unfolded AFS was constructed for the 5-Mb neutralome using 23 ancient individuals with only northern/central European ancestry and 492 haploid modern Dutch individuals. We used ∂a∂i (20) to fit our 2D-AFS based on the model with free demographic parameters as described in Gao and Keinan (46). We performed the analysis using two fixed per generation mutation rates, μ (1.2×10^{-8} and 2.59×10^{-8}) and also allowed μ to be a free parameter. Analyses were performed both with and without transitions. Free parameters were fitted using the Broyden–Fletcher–Goldfarb–Shanno (BFGS) optimizer via a two-step approach.

Functional Markers. Genotypes and phenotypes were determined using the diploid genotyping method described in *SI Appendix*, section 5 and methods described in *SI Appendix*, section 7.

ACKNOWLEDGMENTS. We thank the late Prof. Dr. Živko Mikić for supporting our study and supplying sample material; Andreas Boos and Silvia Codreanu-Windauer for their helpfulness; Heiner Schwarzberg for translation of Russian literature; Patrick Geary for his useful comments; and the Genome of the Netherlands Consortium for access to BAM files. M.H., J. Burger, B.H.-G., A.R., M.G., A.G., and B.T. are supported by Volkswagenstiftung (FKZ 87161); C.S. was supported by Deutsche Forschungsgemeinschaft (BO 4119/1); J. Blöcher was funded by GeneRED; L.v.D. is supported by the Newton Trust (MR/P007597/1); and K.R.V. is supported by National Science Foundation Award 1450606.

1. Halsall G (2007) *Barbarian Migrations and the Roman West, 376-568* (Cambridge Univ Press, Cambridge, UK).
2. Haas-Gebhard B (2013) *Die Baiuvaren: Archäologie und Geschichte* (Pustet, Regensburg, Germany).
3. Tiesler V (2013) *The Bioarchaeology of Artificial Cranial Modifications: New Approaches to Head Shaping and Its Meanings in Pre-Columbian Mesoamerica and Beyond* (Springer Science & Business Media, New York).
4. Dingwall EJ, John E (1931) Later artificial cranial deformation in Europe. *Artificial Cranial Deformation: A Contribution to the Study of Ethnic Mutilations* (Bale, Sons & Danielsson, London), pp 46–80.
5. Werner J (1956) *Beiträge zur Archäologie des Attila-Reiches* (Bavarian Academy of Sciences and Humanities, Munich).
6. Hakenbeck S (2009) "Hunnic" modified skulls: Physical appearance, identity and the transformative nature of migrations. *Mortuary Practices and Social Identities in the Middle Ages*, eds Williams H, Sayer D (Exeter Univ Press, Exeter, UK), pp 64–80.
7. Schröter P (1988) Zur beabsichtigten künstlichen Kopfumformung im völkerwanderungszeitlichen Mitteleuropa. *Die Bajuwaren von Severin Bis Tassilo 488–788*, eds Dannheimer H, Dopsch H (Prähistorische Staatssammlung München und Salzburger Landesregierung, Munich), pp 258–265.
8. Briggs AW, et al. (2007) Patterns of damage in genomic DNA sequences from a Neandertal. *Proc Natl Acad Sci USA* 104:14616–14621.
9. Hofmanová Z, et al. (2016) Early farmers from across Europe directly descended from Neolithic Aegeans. *Proc Natl Acad Sci USA* 113:6886–6891.
10. Trautmann B, et al. (2017) Eine Reevaluation artifiziell deformierter Schädel des Frühen Mittelalters aus Bayern. *Archäologisches Korrespondenzblatt* 47:263–282.
11. Mallick S, et al. (2016) The Simons Genome Diversity Project: 300 genomes from 142 diverse populations. *Nature* 538:201–206.
12. Schiffels S, et al. (2016) Iron Age and Anglo-Saxon genomes from East England reveal British migration history. *Nat Commun* 7:10408.
13. Walsh S, et al. (2013) The HIrisPlex system for simultaneous prediction of hair and eye colour from DNA. *Forensic Sci Int Genet* 7:98–115.
14. Bersaglieri T, et al. (2004) Genetic signatures of strong recent positive selection at the lactase gene. *Am J Hum Genet* 74:1111–1120.
15. Allentoft ME, et al. (2015) Population genomics of Bronze Age Eurasia. *Nature* 522:167–172.
16. Raj T, et al. (2013) Common risk alleles for inflammatory diseases are targets of recent positive selection. *Am J Hum Genet* 92:517–529.
17. Gao F, Keinan A (2016) Explosive genetic evidence for explosive human population growth. *Curr Opin Genet Dev* 41:130–139.
18. Nelson MR, et al. (2012) An abundance of rare functional variants in 202 drug target genes sequenced in 14,002 people. *Science* 337:100–104.
19. Zimmermann A, Hilpert J, Wendt KP (2009) Estimations of population density for selected periods between the Neolithic and AD 1800. *Hum Biol* 81:357–380.
20. Gutenkunst RN, Hernandez RD, Williamson SH, Bustamante CD (2009) Inferring the joint demographic history of multiple populations from multidimensional SNP frequency data. *PLoS Genet* 5:e1000695.
21. Genome of the Netherlands Consortium (2014) Whole-genome sequence variation, population structure and demographic history of the Dutch population. *Nat Genet* 46:818–825.
22. Gazave E, et al. (2014) Neutral genomic regions refine models of recent rapid human population growth. *Proc Natl Acad Sci USA* 111:757–762.
23. Kong A, et al. (2012) Rate of de novo mutations and the importance of father's age to disease risk. *Nature* 488:471–475.
24. Molnár M, János I, Szűcs L, Szathmáry L (2014) Artificially deformed crania from the Hun-Germanic period (5th-6th century ad) in northeastern Hungary: Historical and morphological analysis. *Neurosurg Focus* 36:E1.
25. Kiszely I (1978) *The Origins of Artificial Cranial Formation in Eurasia from the Sixth Millennium BC to the Seventh Century AD* (British Archaeological Reports, Oxford).
26. Unterländer M, et al. (2017) Ancestry and demography and descendants of Iron Age nomads of the Eurasian steppe. *Nat Commun* 8:14615.
27. Scheu A, et al. (2015) The genetic prehistory of domesticated cattle from their origin to the spread across Europe. *BMC Genet* 16:54.
28. Arbiza L, Zhong E, Keinan A (2012) NRE: A tool for exploring neutral loci in the human genome. *BMC Bioinformatics* 13:301.
29. Gronau I, Hubisz MJ, Gulko B, Danko CG, Siepel A (2011) Bayesian inference of ancient human demography from individual genome sequences. *Nat Genet* 43:1031–1034.
30. Jónsson H, Ginolhac A, Schubert M, Johnson PLF, Orlando L (2013) mapDamage2.0: Fast approximate Bayesian estimates of ancient DNA damage parameters. *Bioinformatics* 29:1682–1684.
31. Fu Q, et al. (2013) A revised timescale for human evolution based on ancient mitochondrial genomes. *Curr Biol* 23:553–559.
32. Korneliussen TS, Albrechtsen A, Nielsen R (2014) ANGSD: Analysis of next generation sequencing data. *BMC Bioinformatics* 15:356.
33. Stephens M, Smith NJ, Donnelly P (2001) A new statistical method for haplotype reconstruction from population data. *Am J Hum Genet* 68:978–989.
34. 1000 Genomes Project Consortium; et al. (2015) A global reference for human genetic variation. *Nature* 526:68–74.
35. Alkan C, et al. (2014) Whole genome sequencing of Turkish genomes reveals functional private alleles and impact of genetic interactions with Europe, Asia and Africa. *BMC Genomics* 15:963.
36. Nelson MR, et al. (2008) The population reference sample, POPRES: A resource for population, disease, and pharmacological genetics research. *Am J Hum Genet* 83:347–358.
37. Hellenthal G, et al. (2014) A genetic atlas of human admixture history. *Science* 343:747–751.
38. Patterson N, Price AL, Reich D (2006) Population structure and eigenanalysis. *PLoS Genet* 2:e190.
39. Alexander DH, Novembre J, Lange K (2009) Fast model-based estimation of ancestry in unrelated individuals. *Genome Res* 19:1655–1664.
40. Pritchard JK, Stephens M, Donnelly P (2000) Inference of population structure using multilocus genotype data. *Genetics* 155:945–959.
41. Waser PM, Strobeck C (1998) Genetic signatures of interpopulation dispersal. *Trends Ecol Evol* 13:43–44.
42. Lawson DJ, Hellenthal G, Myers S, Falush D (2012) Inference of population structure using dense haplotype data. *PLoS Genet* 8:e1002453.
43. Delaneau O, Zagury J-F, Marchini J (2013) Improved whole-chromosome phasing for disease and population genetic studies. *Nat Methods* 10:5–6.
44. Nei M (1978) Estimation of average heterozygosity and genetic distance from a small number of individuals. *Genetics* 89:583–590.
45. Bhatia G, Patterson N, Sankararaman S, Price AL (2013) Estimating and interpreting FST: The impact of rare variants. *Genome Res* 23:1514–1521.
46. Gao F, Keinan A (2016) Inference of super-exponential human population growth via efficient computation of the site frequency spectrum for generalized models. *Genetics* 202:235–245.